

# Various Methods for Synthesis of Bulk and Nano Thallium(III) Oxide

Maryam Moeinian<sup>1</sup> · Kamran Akhbari<sup>1</sup>

Received: 6 September 2015 / Accepted: 25 September 2015 / Published online: 3 October 2015  
© Springer Science+Business Media New York 2015

**Abstract** Thallium(III) oxide, a degenerate n-type semiconductor, is a highly insoluble thermally stable thallium source suitable for glass, optic and ceramic applications. Although thallium oxide is an important metal oxide, its synthesis has only been sporadically studied. This review gives an overview of all reported synthetic routes for the preparation of both bulk and nanostructured thallium(III) oxide. These methods include electrochemical methods, thermal method, chemical vapor deposition (CVD), microwave irradiation, sol–gel method and one recently chemical route using potassium superoxide. In electrochemical methods, both bulk and nanostructures of thallium(III) oxide can be prepared and the amount of the deposited material, thickness of the layer or wires length depends on the deposition time matrix structure. Thermal methods are simple and effective techniques which include thermal decomposition and calcination of various precursors. By CVD and microwave irradiation we are able to synthesize bulk and nanostructures of thallium(III) oxide, respectively. A one-step, room temperature, solution synthesis of thallium(III) oxide nanoparticles with a size of about 10 nm is reported by using potassium superoxide.

**Keywords** Chemical vapor deposition · Electrochemistry · Thallium · Nanostructures · Solid-state reactions · Solid-phase synthesis

## Abbreviations

ITO	Indium tin oxide
PsucH	Phenylsuccinic acid
9-HAc	9-Anthracene carboxylic acid
H <sub>2</sub> hpt	5-(4-Hydroxyphenyl)tetrazole
Hbt	5-Phenyltetrazole
Hbbt	5-(4-Bromobenzyl)tetrazole
H <sub>2</sub> bdt	5,5'-Benzene-1,4-diylbistetrazole
Hbet	5-(Benzyl)tetrazole
4-HBN	4-Hydroxy benzonitrile
HTPOAc	Triphenylacetic acid
biphOH	4-Hydroxy biphenyl
2,4-Hdcp	2,4-Dichlorophenol
3,4-Hdcp	3,4-Dichlorophenol
2,5-Hdcp	2,5-Dichlorophenol
2,4,6-Htcp	Trichlorophenol
2,4-Hbcp	2-Bromo-4-chlorophenol
2,4-Hcfp	2-Chloro-4-fluorophenol
4-Hcp	4-Chlorophenol
4-Hip	4-Iodophenol
4-Hfp	4-Fluorophenol
3-np <sup>-</sup>	3-Nitrophenoxide
2,4-dnp <sup>-</sup>	2,4-Dinitrophenoxide
2,4-Hcfp	2-Chloro-4-fluorophenol
CpTl	Cyclopentadienylthallium
Me <sub>2</sub> Tl(acac)	Dimethylthallium acetylacetonate
Tl(acac)	Thallium acetylacetonate
2D	Two-dimensional
3D	Three-dimensional
1D	One-dimensional
ITO	Indium tin oxide
SEM	Scanning electron microscopy
bcc	Body-centered cubic
HRTEM	High-resolution transmission electron microscopy

✉ Kamran Akhbari  
akhbari.k@khayam.ut.ac.ir

<sup>1</sup> School of Chemistry, College of Science, University of Tehran, P.O. Box 14155-6455, Tehran, Islamic Republic of Iran

## 1 Introduction

Thallium reagents, despite their inherent toxicity and cost, have played a conspicuous role in the development of modern inorganic and organometallic chemistry [1–6]. Thallium is generally regarded as toxic, but various thallium compounds have been used for the treatment of ringworm and other skin infections and as a chemical tracer in diagnosis, particularly in cardiology. Thallium compounds are also used for X-ray imaging and infrared detection. Its medical use is limited by a very narrow window between therapeutic and toxic behavior. Thallium is a very important ingredient of many high temperature oxide superconductors, due to the wide range of stoichiometry over which superconductivity is observed in such thallium-doped materials [7].

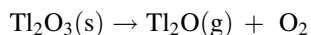
Thallium as a heavy element of group 13 has two oxidation states of +1 and +3. However  $Tl^I$  is a stable ion but coordination polymers of both  $Tl^I$  and  $Tl^{III}$  are studied [4, 8–10]. This was attributed to the effect of the inert pair of electrons, which is generally used in introductory textbooks to explain the tendency of the heavier main group elements to adopt oxidation numbers that are two less than the respective group number. Owing to the relativistic downshift in energy of the 6 s orbital, thallium does indeed favor the oxidation state +1 over +3 [9, 10].

Thallium(I) is formally a low-valence p-block metal with a closed sub-shell ( $s^2$ ) and its chemistry is very interesting due to a variety of reasons: (I) thallium salts or complexes are often anhydrous, (II) the lone pair present on thallium may or may not be stereo-chemically active, (III) high coordination numbers may be present because of the large size of the thallium(I) ion and (IV) because of the ease with which  $Tl(I)$  complexes form metal–metal bonds and also complexes with aromatic hydrocarbons [11, 12]. In  $Tl^+$  ion, When the lone pair appears to have no steric effects, the bonds with ligand (L) donor atoms are arranged throughout the surface of the encompassing sphere (holodirected coordination). Then all the  $Tl-L$  bonds are of intermediate length, and there are no marked differences in the  $Tl-L$  bond lengths.  $Tl(I)$  complexes in which the lone pair is stereo-chemically active, however, have ‘hemidirected coordination’: the  $Tl-L$  bonds are directed only towards a part of the coordination sphere, leaving a gap in the distribution of metal–ligand bonds. The distribution of bond lengths also has a larger distribution: shorter  $Tl-L$  bonds point away from the site of the lone pair and longer  $Tl-L$  bonds are adjacent to the lone pair [13].

On the other hand,  $Tl^I$  favors the formation of neutral species with anionic ligands and it usually favors to forms  $Tl...Tl$ ,  $Tl...C$ ,  $Tl...H$  secondary interactions, especially on its vacant coordination sphere with the stereochemically active lone pair, which indicates that thallium(I) ions

reflect the capacity to act as both a Lewis acid and a Lewis base [14]. Thallium(I) compounds are similar in structure and chemical properties to potassium and silver salts [9, 15].

Coordination chemistry of thallium(III) shows rich geometry and chemical properties in its compounds [16]. The compounds of thallium in its +3 state are easily reduced to compounds of the metal in its +1 state. In its oxidation state of +3, thallium resembles aluminum, although the ion  $Tl^{3+}$  appears to be too large to form alums. It is generally accepted that thallium oxides can adopt one of three structures. The first is that of  $Tl_2O$  the lowest oxide(, a trigonal arrangement of atoms [7, 17]. The second is the monoclinic  $Tl_4O_3$  the mixed-valence oxide) structure [7, 18], and the third is the bixbyite structure (IA3 symmetry) of  $Tl_2O_3$  the highest oxide(, which is a cubic modification of the hexagonal structural arrangement exhibited by the majority of lanthanide oxides [7, 19]. Quite a number of papers have indicated the possibility of other mixed-valence oxides and also thallium oxide compounds formally corresponding to a valence higher than 3 [20]. Thallium(III) oxide is a degenerate n-type semiconductor with a band gap of 1.4 eV [21]. It melts at 716 °C under 1 atm of oxygen [22, 24] and vaporizes in the range 530–675 °C according to following equation [23, 24]:



Thallium(III) oxide is a highly insoluble thermally stable thallium source suitable for glass, optic and ceramic applications. It is black in color and is the inorganic compound of thallium and oxygen. It can also react with acids to make thallium salts. Oxide compounds are not conductive to electricity. However, certain perovskite structured oxides are electronically conductive finding application in the cathode of solid oxide fuel cells and oxygen generation systems. They are compounds containing at least one oxygen anion and one metallic cation. They are typically insoluble in aqueous solutions (water) and extremely stable making them useful in ceramic structures as simple as producing clay bowls to advanced electronics and in light weight structural components in aerospace and electrochemical applications such as fuel cells in which they exhibit ionic conductivity. Metal oxide compounds are basic anhydrides and can therefore react with acids and with strong reducing agents in redox reactions. Thallium Oxide is also available in pellets, pieces, sputtering targets, tablets and nanopowder. Thallium Oxide is generally immediately available in most volumes. Ultra high purity, high purity, submicron and nanopowder forms may be considered. It has electrical and optical properties that make it potentially useful in solar cells and transparent electrical contacts [21, 24].

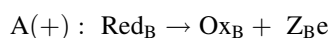
Besides, the synthesis of nano metal oxides with different morphologies has been of significant interest in

material science and industry in the last decade. Nanoparticles that have a diameter of less than 100 nm behave significantly differently from their bulk form. Among them, crystalline and amorphous metal oxides, because of their high surface area, chemical and thermally stable properties, and mesoporous properties, have been extensively studied for catalysts application at high and low temperatures. Nano metal oxides are prepared in very different ways but sometimes the initial product is a metal hydroxide or metal oxhydroxide and this is a limitation in the synthesis of nano thallium oxide, because thallium hydroxide is completely soluble in ordinary solvents such as water, ethanol and methanol [25]. Finally, in this review we decide to study various methods for the synthesis bulk and nanostructures of  $Tl_2O_3$  which include electrochemical methods, thermal method, chemical vapor deposition (CVD), microwave irradiation, sol–gel method and one recently chemical route using potassium superoxide.

## 2 Various Methods for the Synthesis of $Tl_2O_3$

### 2.1 Electrochemical Methods

In general, electrochemical methods may be classified into two types. One is galvanic exchange. Here the potential difference between metals is used to replace one metal layer with another (e.g., in “zincation”). The other is electroless plating where reducing agents are used. The electroless methods are effective because of the simplicity of the apparatus used, and they can be done on complex substrates; last, but not least, the methods are suitable for mass production [26]. Electrolysis is a number of processes taking place in electrolyte and at electrode interfaces while electrical current is applied from external sources. The most important reactions proceed at the interfaces electrode metal/solution. When the electrode is dissolved and in oxide form is present in the solution, this electrode we call anode. The opposite electrode–cathode, is one where ions are reduced and metallic surface is formed. During the electrolysis process, large gradients of ions concentrations are observed. The reactions taking place at the electrodes are described in the following form [27, 28]:



Electrolysis process is a few stage process: (i) ion transportation in electrolyte from one electrode to the opposite one; (ii) chemical reaction with electrical charge transfer at the interface electrode/solution; (iii) other type of surface reactions–adsorption, desorption, crystallization [28]. Electrochemical methods can be divided into the following categories: electrodeposition (electrochemical

deposition) or electrocrystallization and photoelectrochemical deposition. Electrochemical and photoelectrochemical deposition methods for ceramic materials such as thallium(III) oxide are atomic-level architecture techniques. The anhydrous oxide is deposited at room temperature, and the amount of material deposited is related to the anodic coulombs passed. The rate of deposition is precisely controlled by varying the potential in electrochemical deposition, and by varying both the potential and light intensity in photoelectrochemical deposition. Since no thermal treatment is used, the ceramic material can be deposited onto semiconductor substrates such as n-silicon with negligible film/substrate reaction. There is a fundamental difference between electrochemical and photoelectrochemical deposition that has important technological implications. Electrochemical deposition is not a line-of-sight method like physical vapor deposition methods such as sputtering or reactive evaporation. Hence, the electrochemical method has good throwing power, so that complex-shaped substrates and wires can be coated. Photoelectrochemical deposition, however, requires the photogeneration of electron hole pairs in the semiconductor substrate, and is therefore more similar to line-of-sight physical vapor depositions. Photoelectrochemically deposited materials can be patterned on the semiconductor substrates, since the material deposits only on irradiated portions of the electrode [21].

#### 2.1.1 Electrochemical Deposition

Electrodeposition is a method by which ions from the solution are deposited at the surface of the cathode (working electrode). This process can run parallel to electrolysis, and deposited material can form a continuous layer, wires or tubes when prestructured matrixes are used. The amount of the deposited material, thickness of the layer or wires length depends on the deposition time matrix structure [28]. Electrochemically deposited material has in most cases a crystalline structure but the quality of the obtained layers can be different due to the various speeds of crystal growth and crystal seeds creation. Modification of few parameters such as: current density, type and concentration of electrolyte, pH of electrolyte, temperature, presence of surfactants, matrix properties, etc., has significant influence on the quality of deposited material. For each material a range of parameters giving best quality surface can be assigned [28]. Electrochemical deposition is widely used for metallic materials deposition; the method is rather occasionally employed for deposition of III–V compound semiconductors, especially from aqueous solutions. During electrodeposition of semiconductors some challenging task have to be overcome, e.g. higher resistivity of semiconducting deposit and its sensitivity to

crystal lattice defects. These problems are complicated by the fact that resistivity of the deposit can constantly change during electrodeposition [29]. It should be noted that the electrosynthetic and electroanalytical approaches have played a notable role in the history of thallium chemistry. The same could also be said about the modern methods of preparation of semiconducting compounds and high temperature superconductors based on thallium oxide systems. Electrodeposition at room temperature provides relatively safe methods compared with the traditional methods of solid phase synthesis [20]. Recently the electrodeposition of  $Tl_2O_3$  films has been found to be effective for preparing Tl–Pb oxide,  $Tl_2O_3$  super lattices and high-temperature superconducting oxide films [30].

Researchers have used various methods for preparation of  $Tl_2O_3$  by electrodeposition in different studies. For electrodeposition of  $Tl_2O_3$ , Bidattacharya and Pramanik have mixed 15 ml of 1.5 (M/10)  $TlNO_3$  solution with 5 ml of 0.9 (M/10)  $K_2S_2O_8$  solution and 15 ml ammonia liquor. The substrate was placed in the solution and heated to 60–80 °C. A uniform thin film to bulk  $Tl_2O_3$  was obtained. In this case, the borosilicate glasses were found to be the best substrates for uniform deposition. X-ray studies showed that the  $Tl_2O_3$  film was polycrystalline cubic while the scanning electron micrograph showed that the films had a unique deposition pattern [31]. In another work, it has been suggested that there is a possibility of peroxide formation from both strong chemical oxidation and electrolysis of thallos salt solutions. Originally, the composition of the compound obtained by galvanostatic deposition from an oxalate + water + acetone solution was assumed to be  $Tl_3O_5$ . However, the accurate repetition of the experiment showed that under these conditions the peroxide  $TlO_2$  was formed which decomposed in air to  $Tl_2O_3$  and  $O_2$ . The oxidation of  $Tl^+$  to  $Tl_2O_3$  at  $pH > 2-3$  is thermodynamically possible at potentials more negative than the equilibrium potential of the  $H_2O/O_2$  system. However, the pH decrease leads to a dramatic inhibition of the thallium oxide anodic electrocrystallization at a constant over potential. Therefore oxide deposition at  $pH < 10$  could be accomplished only simultaneously with oxygen evolution. In this experiment, as substrates, platinum foils of 0.05–0.5 mm thickness (99.99 wt%Pt), copper foils and plates of 0.1–3 mm thickness (99.9 and 99.999 wt% Cu), plates of glassy carbon and porous graphite (apparent surface area, 0.5–12  $cm^2$ ) were used. Solutions were prepared from electrolytic KOH and NaOH, BaO,  $H_2SO_4$  twice distilled under low pressure and twice-crystallized  $TlCH_3COO$ ,  $TlNO_3$  and  $Tl_2SO_4$  [20]. R. J. Phillips, M. J. Shane, and J. A. Switzer, prepared electrochemically deposited films of thallium(III) oxide onto conducting and p-type semiconducting substrates. Thallium(I) acetate was used for the depositions. In this study the redox change

method is used, since the thallium(I) ion is oxidized to thallium(III) oxide. Single crystal (100) wafers of semiconductor-grade n-silicon were obtained from Monsanto. The wafers were doped with phosphorus by the manufacturer to a volume resistivity of 2.1–2.4  $\Omega\text{-cm}$ . Back ohmic contacts were made either with Ga–In eutectic or by evaporating a thin film of aluminum onto a cooled silicon substrate. Platinum, stainless steel, and silicon working electrode areas were 1.0  $cm^2$  in all cases. The semiconductor electrodes were irradiated with an Oriol Model 6431 250 W quartz tungsten-halogen source. Melles Griot 10 nm bandwidth interference filters were used for monochromatic light experiments. These results show that the films grow with cube faces parallel to the electrode surface [21]. In another work,  $Tl_2O_3$  films were electrodeposited onto ITO substrates at different current densities. For repeated uses, the  $Tl_2O_3$  films were dissolved in an aqueous solution of ascorbic acid and rinsed with deionized, twice-distilled water. The electrodeposition solution was 1.00  $mol\ dm^{-3}$  KOH containing 0.18  $mol\ dm^{-3}$  TlAc and deionized, twice-distilled water was used to prepare the solution. To measure the resistivity of the  $Tl_2O_3$  films, Au sputtering on top or two sides of the film was performed on a LDM 150 ion sputtering equipment. All the experiments were performed at room temperature (about 208 °C). The resultant films are amorphous at low electrodeposition current densities, while polycrystalline films are obtained at high electrodeposition current densities. In contrast with the amorphous film, the polycrystalline film assumes granular growth at a preferred orientation, and has a lower resistivity than the amorphous one. The polycrystalline to amorphous transformation takes place when the electrodeposition current density increases to 0.70–0.75  $mA\ cm^{-2}$ . The XRD analysis demonstrates that the electrodeposited  $Tl_2O_3$  film can be either polycrystalline or amorphous depending on the deposition current density [32]. The polycrystalline and amorphous  $Tl_2O_3$  films exhibit different surface and cross-section morphologies. According to the XRD analysis, the amorphous film consists of  $Tl_2O_3$  nanoparticles with a size of about 1.2 nm. The thickness of the polycrystalline film is also different from that of the amorphous one under the same electrodeposition charge conditions. Figure 1 shows that thickness of the amorphous film is greater, suggesting that it contains a higher content of excess Tl and more pores than the polycrystalline film [30].

### 2.1.2 Photoelectrochemical Deposition

In photoelectrochemical experiments, irradiation of an electrode with light that is absorbed by the electrode material causes the production of a current (a photocurrent). The dependence of the photocurrent on wavelength,



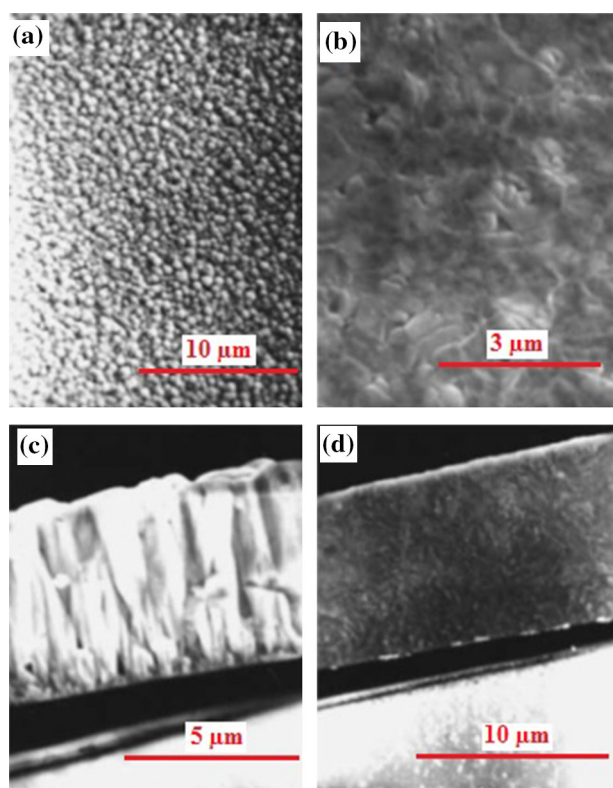


**Fig. 1** Scanning electron micrographs of  $\text{Tl}_2\text{O}_3$  films electrodeposited at **a, c** 20 and **b, d** 0.10  $\text{mA cm}^{-2}$ , in 1.00  $\text{mol dm}^{-3}$  KOH containing 0.18  $\text{mol dm}^{-3}$  TlAc. Electrodeposition charge: **a, b** 1.00 and **c, d** 10.0  $\text{C cm}^{-2}$ . Reproduced with permission of Elsevier

electrode potential, and solution composition provides information about the nature of the photoprocess, its energetics, and its kinetics. Photocurrents at electrodes can also arise because of photolytic processes occurring in the solution near the electrode surface. Photoelectrochemical studies are frequently carried out to obtain a better understanding of the nature of the electrode-solution interface. However, because the production of a photocurrent can represent the conversion of light energy to electrical and chemical energy, such processes are also investigated for their potential practical applications. Consideration of semiconductor electrodes also helps in gaining a microscopic understanding of electron-transfer processes at solid-solution interfaces [33]. Semiconductor electrodes tend to form rectifying junctions with solutions, due to the energetic mismatch of the Fermi level of the semiconductor and the electrochemical potential of the solution. In general, n-type semiconductors are rectifiers toward anodic processes, and p-type semiconductors are rectifiers toward cathodic processes [21, 34–36].

About photoelectrochemical deposition of  $\text{Tl}_2\text{O}_3$ , Phillips, Shane and Switzer, have deposited photoelectrochemically a bulk thallium(III) oxide onto n-silicon(n-type

semiconducting substrates) in an anodic process. Thin films were grown by irradiating the n-silicon with 450 nm monochromatic light, since the light was strongly absorbed by the thallium(III) oxide. The most uniform thin films were deposited when the n-silicon was initially irradiated with a short pulse of high intensity light. The scanning electron micrograph of the film that was grown by irradiation with 450 nm light is shown in Fig. 2. The electrode was irradiated with 6.8  $\text{mW/cm}^2$  light for a total time of 42 min and coverage of 0.5  $\text{coulomb/cm}^2$ . The film is fairly uniform, and is composed of small 0.2  $\mu\text{m}$  spheres. The thickness is approximately equal to the sphere diameters. Hence, the photoelectrochemical deposition is “turned-off” through light attenuation after the electrode is covered with a thin film. In the photoelectrochemical deposition of hundreds of thallium(III) oxide films, the most uniform thin ( $\sim 0.1 \mu\text{m}$ ) films of thallium(III) oxide are deposited when the n-silicon is initially irradiated with a short pulse of high intensity light. The pulse apparently promotes the instantaneous nucleation of a high density of thallium(III) oxide nuclei [21].

## 2.2 Thermal Methods

Thermal methods are simple and effective techniques which include thermal decomposition and calcination [37–43]. Thermal decomposition, or thermolysis, is a chemical decomposition caused by heat [44–51]. The decomposition temperature of a substance is the temperature at which the substance chemically decomposes. The reaction is usually endothermic as heat is required to break chemical bonds in the compound undergoing decomposition. If decomposition is sufficiently exothermic, a positive

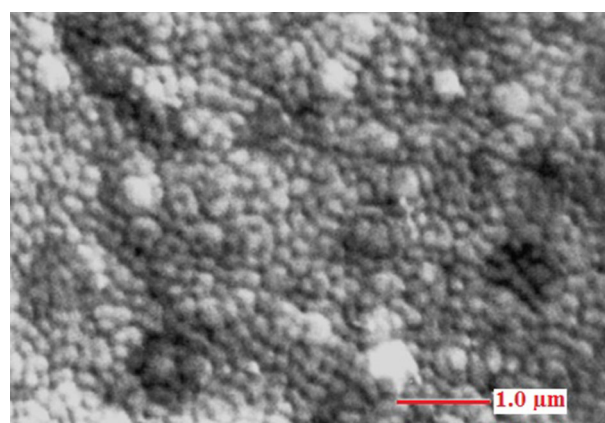


**Fig. 2** Scanning electron micrograph of thallium(III) oxide film grown with 450 nm light at an irradiance of 6.8  $\text{mW/cm}^2$ . Substrate is n-Si. Potentiostated at +0.5 V vs SCE. Initial irradiation with 3000  $\text{mW/cm}^2$  tungsten-halogen light to 0.025  $\text{coulomb/cm}^2$ . Stirred alkaline solution (1.0 M NaOH, 0.2 M  $\text{Tl}^+$ ). Marker on micrograph is 1.0  $\mu\text{m}$ . Reproduced with permission of Materials Research Society

feedback loop is created producing thermal runaway and possibly an explosion. When metals are near the bottom of the reactivity series, their compounds generally decompose easily at high temperatures. This is because stronger bonds form between atoms towards the top of the reactivity series, and strong bonds break less easily. For example, copper is near the bottom of the reactivity series, and copper sulfate ( $\text{CuSO}_4$ ), begins to decompose at about  $200\text{ }^\circ\text{C}$ , increasing rapidly at higher temperatures to about  $560\text{ }^\circ\text{C}$ . In contrast potassium is near the top of the reactivity series, and potassium sulfate ( $\text{K}_2\text{SO}_4$ ) does not decompose at its melting point of about  $1069\text{ }^\circ\text{C}$ , nor even at its boiling point. Calcination is a thermal treatment process applied to ores and other solid materials to bring about a phase transition or removal of a volatile fraction.

In this regard, Mohammadi et al. were synthesized a 1D thallium(I) coordination polymer,  $[\text{Tl}(2,4,6\text{-tcp})]_n$  (**1**). The thallium ions in this compound may be considered five-coordinate, the resulting environment being as  $\text{TlO}_3\text{Tl}_2$  [12, 52]. In **1**, the lone pair of  $\text{Tl}^{\text{I}}$  atoms is “active” in the solid state. In order to preparation of  $\text{Tl}_2\text{O}_3$  nanostructures from this precursor,  $0.2\text{ mmol}$  of **1** was dissolved immediately in oleic acid ( $1.35\text{ mL}$ ). This solution was heated to  $280\text{ }^\circ\text{C}$  for  $2\text{ h}$  in an air atmosphere. At the end of the reaction, a black precipitate was formed. A small amount of toluene and a large excess of MeOH were added to the reaction solution and  $\text{Tl}_2\text{O}_3$  nanostructure was separated by centrifugation. Finally they could prepare nanorods structure of  $\text{Tl}_2\text{O}_3$  by this process (Fig. 3) [12].

In another work, a 2D thallium(I) coordination polymer  $[\text{Tl}(\text{PsucH})]_n$  (**2**), has been synthesized and characterized by single crystal X-Ray analysis, elemental analysis and IR spectroscopy. There is only one thallium atom with coordination number of 8. It seems that the  $6s^2$  lone pair electron of thallium is inactive in this polymer. No secondary interaction of  $\text{Tl}\dots\text{Tl}$ ,  $\text{Tl}\dots\text{H}$  and  $\text{Tl}\dots\text{C}$  exists in its structure too. Calcination of **2** was occurred at  $600\text{ }^\circ\text{C}$  under air atmosphere. As a result, the whole organic component of it was combusted and the thallium(III) oxide nanostructure with nano flowerlike morphology was produced (Fig. 4) [53].

$[\text{Tl}_2(\mu_3\text{-9-Ac})(\mu_4\text{-9-Ac})(\text{H}_2\text{O})]_n$  (**3**), is a 2D thallium(I) supramolecular polymer, which contains two types of thallium(I) ions with  $\text{O}_5\text{Tl}^{\text{I}}\dots\text{C}_5$  and  $\text{O}_4\text{Tl}^{\text{I}}\dots\text{C}_5$  coordination spheres. The lone pairs of the  $\text{Tl}^{\text{I}}$  ions are ‘active’ in the solid state. The bulk and micro-rods samples of **3** were used for preparation of  $\text{Tl}_2\text{O}_3$  nanostructures. These two samples were calcined at  $495\text{ }^\circ\text{C}$  in a furnace under a static atmosphere of air for  $5\text{ h}$ . The difference between the morphology of the two  $\text{Tl}_2\text{O}_3$  nanostructures originated from the different morphology of initial precursors of **3** [54]. In another work, a 1D thallium(I) coordination polymer,  $[\text{Tl}_2\text{hpt.H}_2\text{O}]_n$  (**4**), was synthesized and

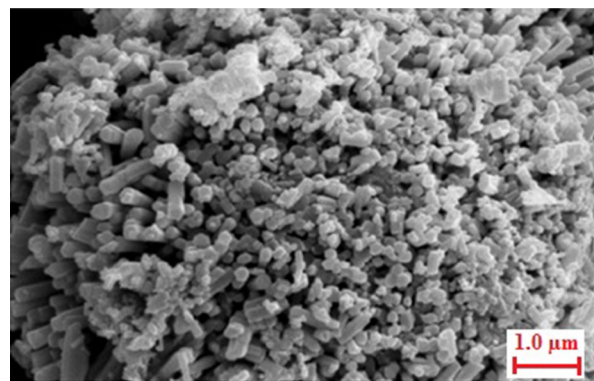


**Fig. 3** SEM micrograph of  $\text{Tl}_2\text{O}_3$  nanorods produced by thermal decomposition of compound  $[\text{Tl}(2,4,6\text{-tcp})]_n$  (**1**) in oleic acid. Reproduced with permission of John Wiley & Sons

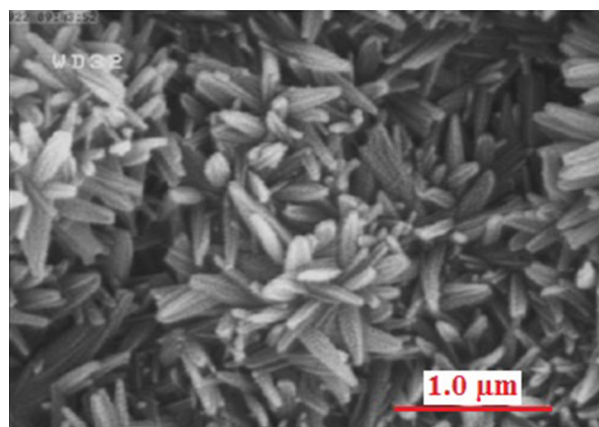


**Fig. 4** The SEM image of  $\text{Tl}_2\text{O}_3$  nanorods produced by calcination of  $[\text{Tl}(\text{PsucH})]_n$  (**2**). Reproduced with permission of Springer

characterized by X-ray crystallography. There are two types of  $\text{Tl}^{\text{I}}$  ions in this polymeric compound. They have  $\text{NO}_2\text{Tl}\dots\text{C}_2$  coordination spheres with electrochemically active electron lonepair. For preparation of  $\text{Tl}_2\text{O}_3$ ,  $1\text{ mmol}$  of compound **4** was placed in a furnace and heated to  $450\text{ }^\circ\text{C}$  for  $4\text{ h}$ . After cooling,  $\text{Tl}_2\text{O}_3$  was obtained as a black precipitate. The morphology, structure, and size of the resulting  $\text{Tl}_2\text{O}_3$  nanoparticles were investigated by SEM [10].  $[\text{TlBt}]_n$  (**5**),  $[\text{TlBbt}]$  (**6**),  $[\text{Tl}_2\text{Bdt}]_n$  (**7**) and  $[\text{TlBet}]$  (**8**) are four thallium(I) coordination polymers, which have been synthesized and characterized by Yazdanparast et al. The Tl ions in compound **5** have a  $\text{TlN}_3$  coordination sphere with electrochemically active electron lonepair. The structures of compounds **6–8** are similar to **5** with the same interactions, except in the distance of the interactions. The tetrazolate and phenyl rings are arrayed in a way that the Tl ion in **8** has secondary interactions with the carbon atoms of the phenolic ring. For preparation of the  $\text{Tl}_2\text{O}_3$  nanostructures, about  $500\text{ mg}$  of compounds **5–8** was heated to  $450\text{ }^\circ\text{C}$  for  $4\text{ h}$ . After cooling,  $\text{Tl}_2\text{O}_3$  as a

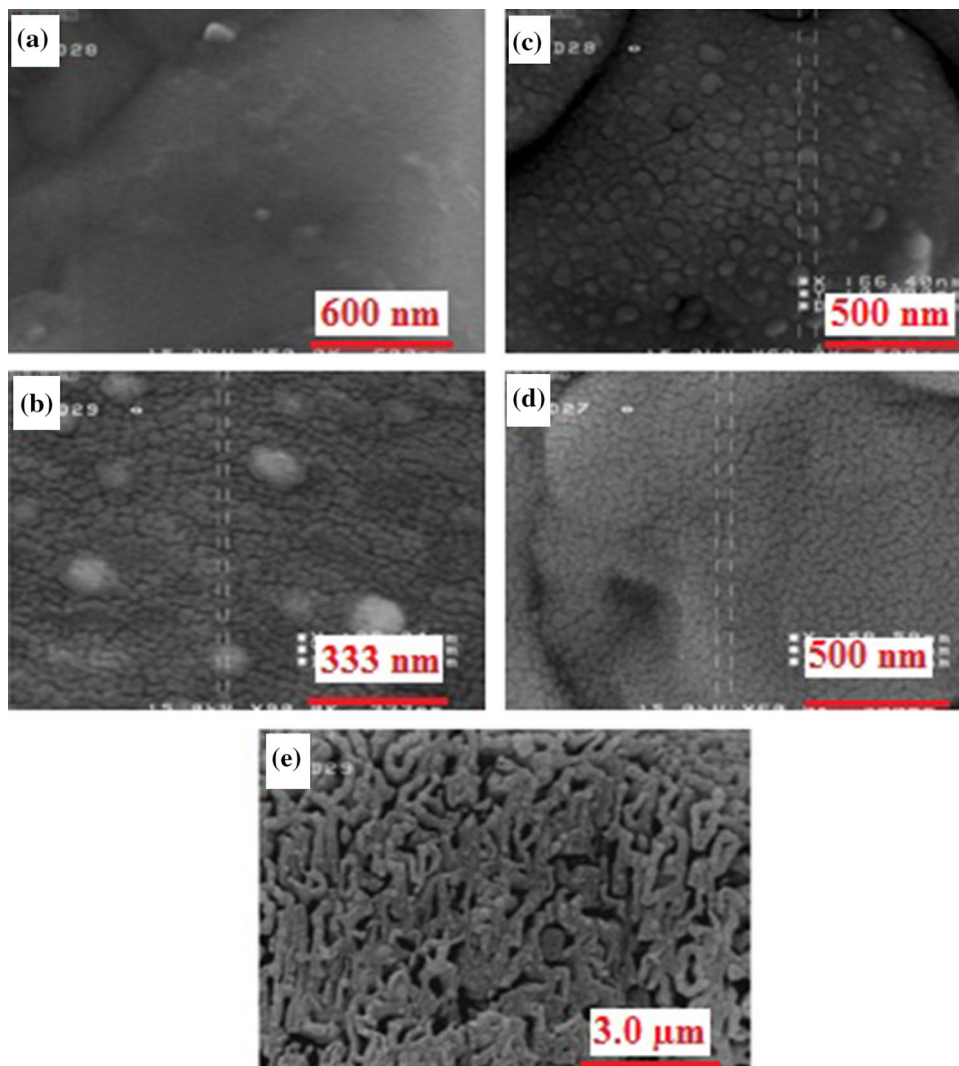
black precipitate was obtained. Figure 5 shows the SEM image of the  $Tl_2O_3$  nanoparticles, which were obtained from simple calcination of compounds **5–8** [25].

$[Tl_4(\mu_3-4-BN)_4]_n$  (**9**) is another thallium(I) supramolecular polymer with a disordered cubic cage structural unit. Four  $Tl^+$ -ions with coordination sphere of  $O_3Tl \dots NTl_2$  exist in **9**. The arrangement of O atoms suggests a gap or hole in the coordination geometry around the Tl(I) center, a gap possibly occupied by a ‘stereoactive’ electron lone pair. Utilizing water-in-oil microemulsion-based methodology for synthesis of **9**, results in formation a mixture of TlBr nanoballs and nanorods. In addition, a fine powder of compound **9** and TlBr nanostructures were used for the preparation of  $Tl_2O_3$  nanostructures. A fine powder of compound **9** was calcined at 470 °C in a furnace and under a static atmosphere of air for 5 h. SEM images of the residue obtained from calcination of compound **9** fine powder at 470 °C showed that thallium(III) oxide with a nanostructural surface was formed. Also in order to obtain

$Tl_2O_3$  nanostructures from TlBr nanostructures, this precipitate was calcined at 600 °C in a furnace and under a static atmosphere of air for 5 h. The SEM images of black fine powder shows the formation of cubic  $Tl_2O_3$  structures with a nanostructural surface (Fig. 6) [55].

In another work, micro and nanostructures of a 2D thallium(I) supramolecular polymer,  $[Tl_2(\mu_3-TPOAc)(\mu_4-TPOAc)]_n$  (**10**), were synthesized by sonochemical methods. Determination the structure of this compound by X-ray crystallography showed the compound is a dimer with two types of  $Tl^+$ -ions. The complex can be considered to contain thallium(I) ions with  $O_5Tl(1) \dots C_3$  and  $O_2Tl(1A) \dots C_2$  coordination spheres. The lone pair of the Tl(I) ions is ‘active’ in the solid state, too. In order to preparation of  $Tl_2O_3$  from compound **10** precursor, the fine powder of its nanostructures which fabricated from sonochemical process, were calcined at 600 °C. SEM images of the residue, shows that thallium(III) oxide with nanostructural surface was formed [56].  $[Tl_6(biphO)_4(biphOH)_4(NO_3)_2]_n$  (**11**) is a 2D

**Fig. 5** a–d) The SEM images of  $Tl_2O_3$  nanoparticles and e) microstructure produced by the calcination of compounds **5–8**, respectively. Reproduced with permission of Royal Society of Chemistry





supramolecular polymer which has three types of Tl ions. Intra-plane hydrogen bonding network also exists in **11**. In compound **11**, the lone pair of Tl(I) ions is 'active' in the solid state and the complex can be considered to contain thallium(I) ions with  $O_3Tl1...O_2$ ,  $O_1Tl2...C_6$  and  $O_3Tl3...O_2$  coordination spheres. Two different morphologies of  $Tl_2O_3$  were produced by direct calcination of **11** at 430 and 570 °C in a furnace and static atmosphere of air for 5 h. The whole of organic components were combusted and the thallium(III) oxide nanostructures were produced. Figure 7 shows SEM images of produced  $Tl_2O_3$  nanostructures by direct thermolyses method. The morphology and size of the nanostructures became different in the two different temperatures. The prepared  $Tl_2O_3$  by the direct calcination at 430 and 570 °C has particle shaped nanostructure (Fig. 7a) and nano rods morphology (Fig. 7b), respectively. Comparison between these two results indicates that with increase in temperature, the small nano particles (Fig. 7a) were grown and finally  $Tl_2O_3$  nano rods (Fig. 7b) were formed at 570 °C. It seems that by increase in temperature, the small nano

particles were grown and finally  $Tl_2O_3$  nano rods were formed at 570 °C [14].

In another work, structural determination of compounds  $[Tl_4(\mu_3-2,4-dcp)_4]$  (**12**),  $[Tl_4(\mu_3-3,4-dcp)_4]$  (**13**),  $[Tl(\mu_3-2,5-dcp)]$  (**14**),  $[Tl_4(\mu_3-2,4-bcp)_4]$  (**15**),  $[Tl_4(\mu_3-4-cp)_4]$  (**16**),  $[Tl_4(\mu_3-4-ip)_4]$  (**17**) and  $[Tl(\mu_3-4-fp)]$  (**18**) by X-ray crystallography showed that we could divide these compounds into three groups upon the three types of primary structural units; group (I) with a distorted tetranuclear cubic cage unit, which could be observed in compounds **12**, **13**, **15**, **16** and **17**, group (II) with a dimeric unit, which could be observed in compound **14** and group (III) with a butterfly dimeric unit, which could be observed in compound **18**. The Thallium(I) complexes of group I have three coordinated  $Tl^I$  ions with a  $TlO_3$  coordination sphere and the thallium(I) complexes of groups II and III have two coordinated  $Tl^I$  ions with a  $TlO_2$  coordination sphere. Secondary thalophilic interactions which exist in **12**, extend the coordination sphere of it to  $O_3Tl...Tl_2$ . Compound **13** is a 2D supramolecular polymer which has two types of  $Tl^I$  ions with  $O_3Tl1...Tl_2C$  and  $O_3Tl2...Tl_2$  coordination spheres. The structure, thallium(I) coordination sphere,

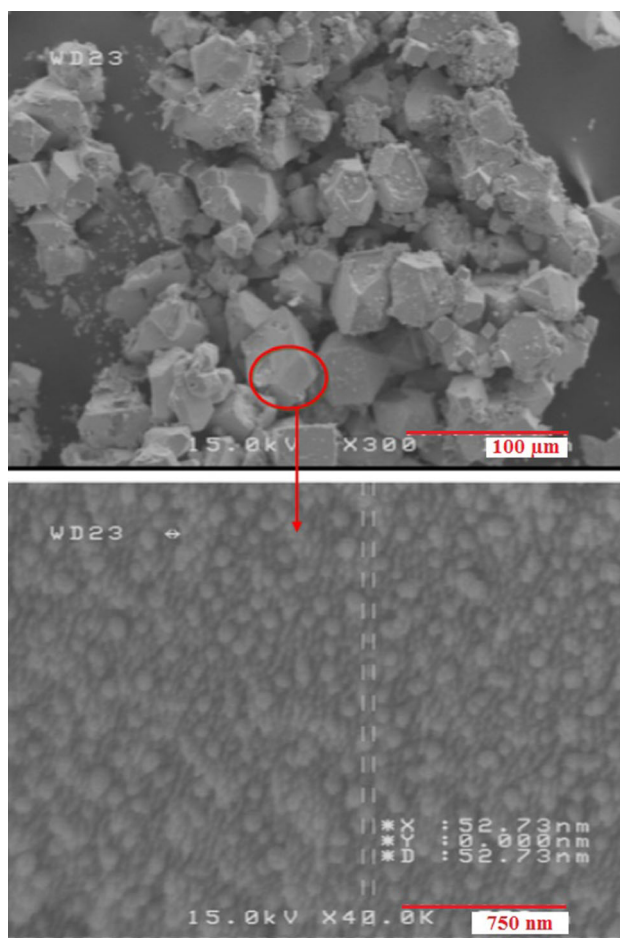


**Fig. 6** SEM images of the  $Tl_2O_3$  nanostructural surface, prepared by calcination of  $TlBr$  nanostructures at 600 °C. Reproduced with permission of Elsevier

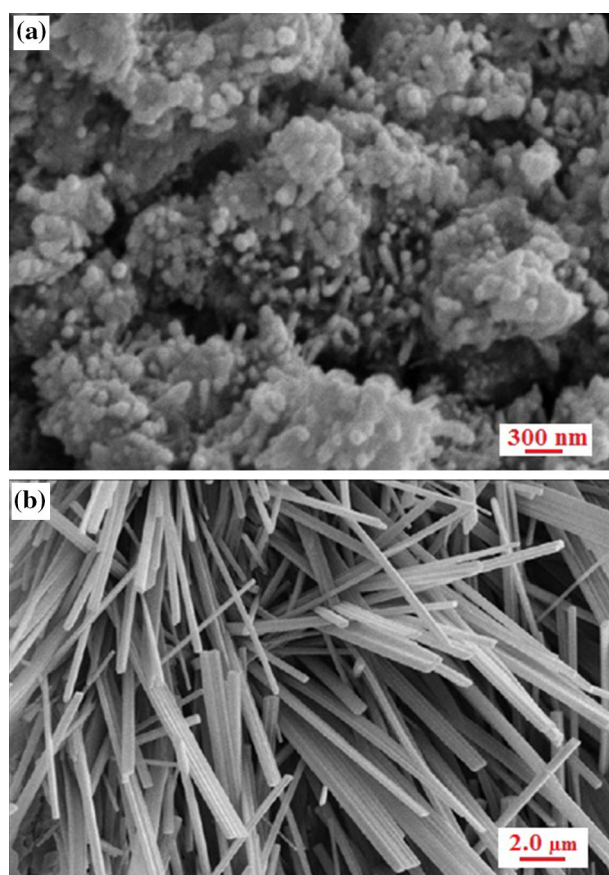


**Fig. 7** SEM micrograph of  $Tl_2O_3$  nanostructures produced by direct calcination of compound **11** at **a** 430 °C and **b** 570 °C, respectively. Reproduced with permission of Elsevier



crystal system and space group of **15** is completely similar to **12**. Compound **16** is a 3D supramolecular polymer with  $\text{Tl}^{\text{I}}$  coordination spheres of  $\text{O}_3\text{Tl}\dots\text{C}_6\text{ClTl}_2$ . Compound **17** has four types of  $\text{Tl}^{\text{I}}$  ions. Some Tl ions in **17** have secondary interactions with carbon atoms of the adjacent phenolic ring. These secondary  $\text{Tl}\dots\text{C}$  interactions result in the formation of a 3D supramolecular network in **17**. In addition, short  $\text{Tl}\dots\text{I}$  contacts also exist in **17**, which is another agent in the formation of the 3D network in this compound. Compound **14** from group II is a 1D stair like coordination polymer. Secondary intrachain interactions of  $\text{Tl}\dots\text{C}$ ,  $\text{Tl}\dots\text{Tl}$  and  $\text{Tl}\dots\text{H}$  also exist in **14**. This compound can be also considered as a 3D supramolecular network with a  $\text{Tl}^{\text{I}}$  coordination sphere of  $\text{O}_3\text{Tl}\dots\text{C}_2\text{Cl}_3\text{Tl}_3\text{H}$ . Group III of thallium(I) complexes with a butterfly dimeric unit only consists of compound  $[\text{Tl}(\mu_3\text{-4-fp})]$  (**18**). This compound also has a 1D structure and Tl atoms are coordinated with three phenolic oxygen atoms. Secondary intrachain  $\text{Tl}\dots\text{C}$  interactions also exist in **18**. Thus, compound **18** is a 1D coordination polymer with intra-chain  $\text{Tl}\dots\text{C}$  interactions and an  $\text{O}_3\text{Tl}\dots\text{C}_6$  coordination sphere. In order to obtain  $\text{TlCl}$  and  $\text{Tl}_2\text{O}_3$  nanostructures, the fine powder of each compounds (**12–18**) obtained after grinding single crystals of them, were calcined at 600 °C in a furnace and static atmosphere of air for 5 h, except for compounds **12** and **18**, which were fired at 580 and 400 °C, respectively. White powders of  $\text{TlCl}$  were obtained from compounds **12–16**, but the calcination process on compounds **17** and **18** results in the formation of  $\text{Tl}_2\text{O}_3$  black powder. Figure 8 shows SEM images of the produced  $\text{TlCl}$  and  $\text{Tl}_2\text{O}_3$  nanostructures from the calcination process of compounds **12** at 580 °C, **13–17** at 600 °C and compound **18** at 400 °C. These SEM images show the formation of  $\text{TlCl}$  and  $\text{Tl}_2\text{O}_3$  nanostructures from the above  $\text{Tl}^{\text{I}}$  supramolecular compounds [57].

Mohammadi et al. were also reported two 3D thallium(I) coordination polymers of  $[\text{Tl}(3\text{-np})]$  (**19**) and  $[\text{Tl}(2,4\text{-dnp})]$  (**20**). Then these two compounds were calcined at 600 °C under air atmosphere. The whole of organic components were combusted and the thallium(III) oxide nanostructures were produced. SEM images show the flowerlike and nanopowder  $\text{Tl}_2\text{O}_3$  nanostructures produced by calcination of **19** and **20**, respectively. The morphology and size of the particles are different in the two samples obtained from two different coordination polymers [52]. In another work, a three-dimensional supramolecular polymer of  $[\text{Tl}_4(\mu_3\text{-2,4-cfp})_4]$  (**21**) was used for preparation of  $\text{Tl}_2\text{O}_3$  nanostructures. It has four types of  $\text{Tl}^{\text{I}}$  ions with  $\text{O}_3\text{Tl}\dots\text{C}_6\text{Tl}_2$ ,  $\text{O}_3\text{Tl}_2\dots\text{TlClF}$ ,  $\text{O}_3\text{Tl}_3\dots\text{Tl}_2$  and  $\text{O}_3\text{Tl}_4\dots\text{C}_2\text{TlH}$  coordination spheres. In order to obtain  $\text{Tl}_2\text{O}_3$  nanostructures, well-ground single crystals of **21** were calcined at 570 and 630 °C in a furnace with static air for 5 h. SEM images of the residue obtained

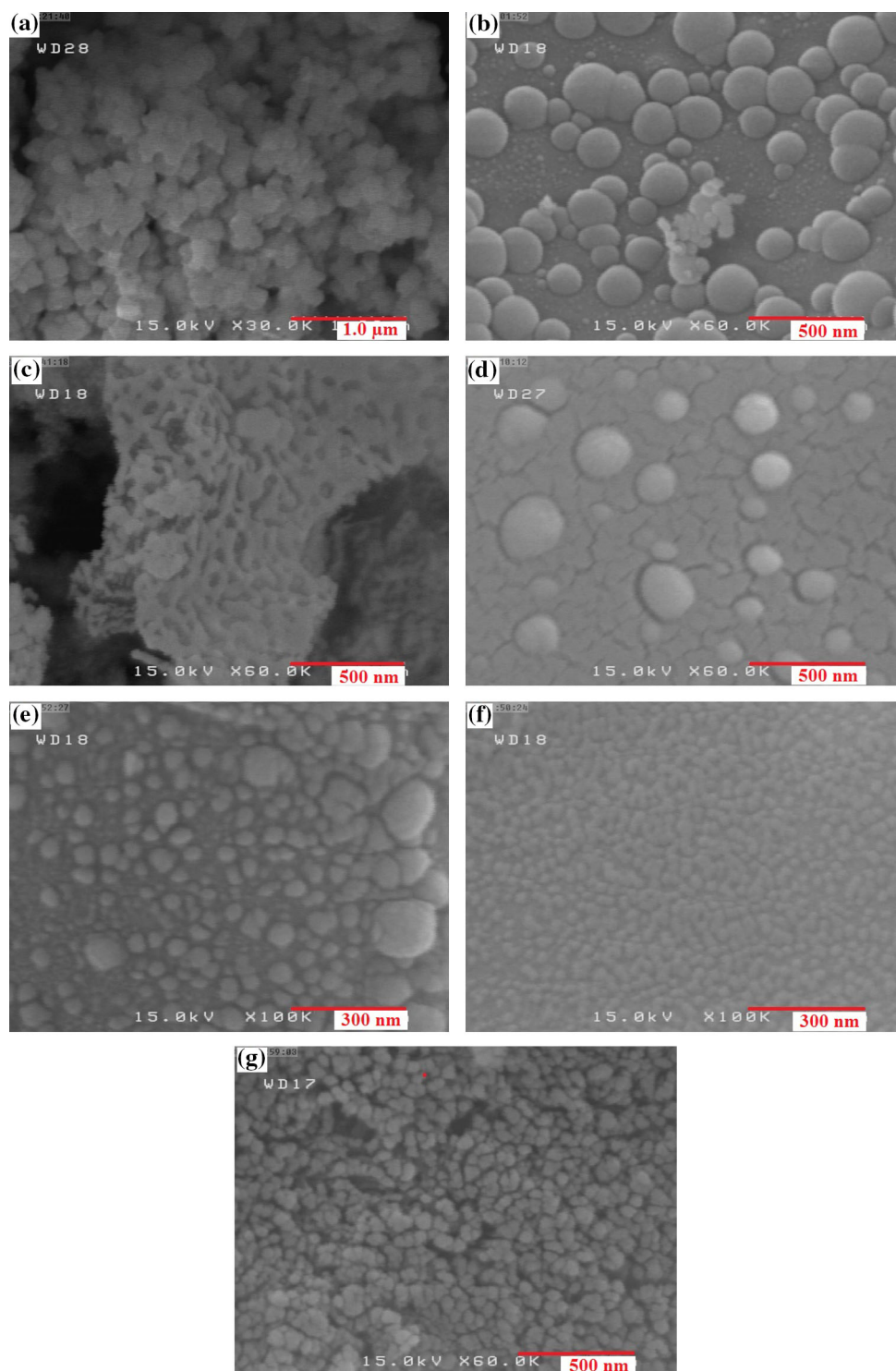
from calcination of fine powders of **21** at 570 °C show that nanostructures of  $\text{Tl}^{\text{III}}$  oxide are formed. If the calcination process were done at 630 °C,  $\text{Tl}_2\text{O}_3$  nanoflowers were formed (Fig. 9). Comparison between these two results indicates that with increase in temperature, small nanostructures are grown; and, finally  $\text{Tl}_2\text{O}_3$  nanoflowers (Fig. 9) are formed at 630 °C [58].

Lyons et al. were performed similar investigations directed toward the preparation of the common IA3 phase of thallium oxide by thermal decomposition of thallium nitrate. This process led to the synthesis of novel and previously undescribed thallium oxide phases under controlled conditions. An unexpected material with a perovskite-like  $\text{MMO}_3$  ( $\text{M} = \text{Tl}^{3+}$ ) structure was formed. Samples were prepared from 0.5 M solutions of thallium nitrate. The solutions were dried at 60 °C overnight and calcined in air at 300 °C for 8 h in silica crucibles. Portions of the solid obtained were calcined in air for 6 h at temperatures of 400, 500, 600, 700, 800, 900, and 1000 °C. At calcination temperatures of 700 °C and above only some 1–10 % of the initial material is present after 6 h. It is believed that the expected phase is formed because complete reduction to metal occurs at these temperatures and air oxidation leads to formation of the  $\text{Tl}_2\text{O}_3$  phase [7].

### 2.3 Chemical Vapor Deposition (CVD)

Chemical vapor deposition (CVD) is a widely used materials-processing technology. The majority of its applications involve applying solid thin-film coatings to surfaces, but it is also used to produce high-purity bulk materials and powders, as well as fabricating composite materials via infiltration techniques. It has been used to deposit a very wide range of materials. The majority of the elements in the periodic table have been deposited by CVD techniques, some in the form of the pure element, but more often combined to form compounds. In its simplest incarnation, CVD involves flowing a precursor gas or gases into a chamber containing one or more heated objects to be coated. Chemical reactions occur on and near the hot surfaces, resulting in the deposition of a thin film on the surface. This is accompanied by the production of chemical by-products that are exhausted out of the chamber along with unreacted precursor gases. As would be expected with the large variety of materials deposited and the wide range of applications, there are many variants of CVD [59]. As an example, we can refer to the research done by Berry et al. in which Films containing thallium(III) oxide were grown by organometallic CVD in an oxygen-rich atmosphere on  $\text{MgO}$ ,  $\text{Al}_2\text{O}_3$ , and Si substrates. They were used three organothallium precursors: thallium acetylacetonate, dimethylthallium acetylacetonate, and cyclopentadienylthallium. Film depositions were carried out at ambient

**Fig. 8** SEM images of TlCl; **a 12, b 13, c 14, d 15, e 16** and  $\text{Tl}_2\text{O}_3$ ; **f 17 and g 18** nanostructures, prepared by the calcination process of the related compounds. Reproduced with permission of Royal Society of Chemistry



pressure in a vertical Pyrex reactor. Precursor transport lines were wrapped with heater tape and source temperatures varied in the ranges 125–130 °C for  $\text{CpTl}$ , 135–140 °C for  $\text{Me}_2\text{Tl}(\text{acac})$  and 140–145 °C for  $\text{Tl}(\text{acac})$ . Nitrogen was passed over the heated precursors at 150  $\text{cm}^3/\text{min}$  and mixed with oxygen flowing at 1000  $\text{cm}^3/\text{min}$  prior to entering the reactor [24].

## 2.4 Microwave Irradiation

The rapid heating of food in the kitchen using microwave ovens prompted a number of scientists engaged in different disciplines to explore the potential of microwave technology in a number of useful processes. These include the preparation of samples for analysis; application to waste

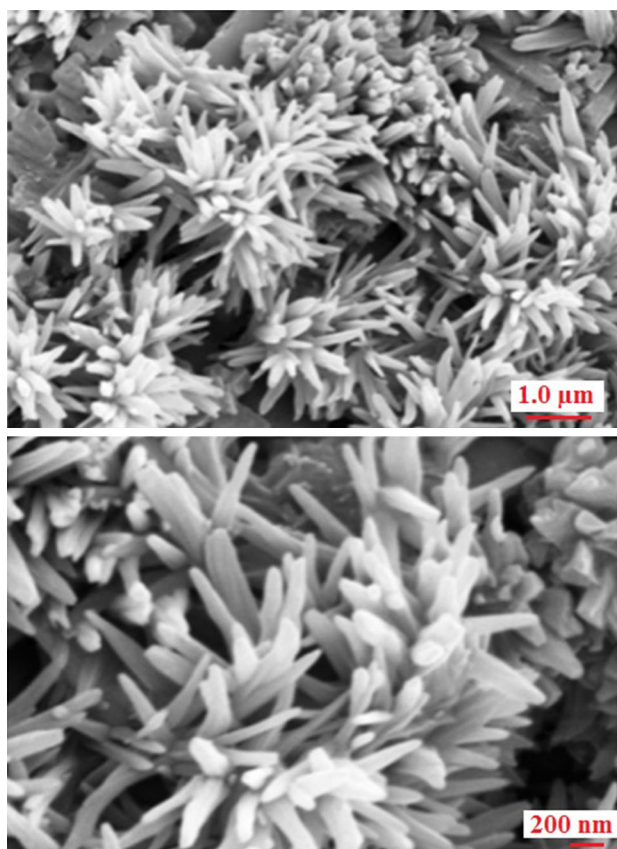


**Fig. 9** SEM image of  $\text{Tl}_2\text{O}_3$  nanoflowers prepared by calcination of **21** at  $630\text{ }^\circ\text{C}$ . Reproduced with permission of Springer

treatment; polymer technology; drug release or targeting; ceramics; alkane decomposition, etc. Microwaves form a part of the electromagnetic spectrum with the wavelength lying between 1 cm and 1 m. In order to avoid interference with radar and telecommunication activities, which also operate in this region, most commercial and domestic microwave ovens operate at 2450 MHz (12.25 cm). The ability of a material to convert electromagnetic energy into thermal energy is dependent on the dielectric constant coupling with microwaves [60]. The microwave-assisted products are pure, structurally uniform, and highly crystalline and are obtained in high yield; furthermore, this method does not need high temperature, high pressure, any catalyst, template, surfactant, vacuum conditions or pre-processing. Additionally, this method is simple, fast, clean, efficient, cheap, economical, non-toxic, and eco-friendly. It also may be extended to fabricate many other nanoscale materials. For example, microwave heating provides an effective and rapid method for the synthesis of nanocrystalline  $\text{Tl}_2\text{O}_3$  powders because of its homogeneous and fast-heating characteristics. In these reactions the temperature is a dominant factor in affecting the reactivity. As an

example, we can refer to the research done by C. R. Patra and A. Gedanken in which “Semiconducting nanoparticles of  $\text{Tl}_2\text{O}_3$  have been successfully synthesized in high yield (>95 %) by microwave irradiation”. In their work, 0.310 g (1 mM) thallium(III) chloride salts in 40 g of distilled water were placed in a 100 ml round-bottomed flask and then 10 ml of the ammonium hydroxide solution was added. The sample was irradiated simultaneously for 60 min, without further addition of the ammonia solution, with 60 % of the instrument’s power in open air atmosphere. The as-synthesized material was a crystalline bcc phase of  $\text{Tl}_2\text{O}_3$ . The particles are of uniform size, being about 16 nm for  $\text{Tl}_2\text{O}_3$ . Figure 10a shows an HRTEM image revealing the general morphology of as-synthesized crystalline  $\text{Tl}_2\text{O}_3$ . It can be seen that the sample consists of mainly spherical nanoparticles of a diameter of 15–16 nm. A representative HRTEM image (Fig. 10b) of a single spherical particle of as-synthesized  $\text{Tl}_2\text{O}_3$  shows the lattice planes with a clearly resolved interplanar distance of  $d_{222} = 0.31\text{ nm}$ , compared with a theoretical interplanar spacing of 0.3042 nm [61].

## 2.5 Sol–Gel Method

A sol is a dispersion of the solid particles ( $\sim 0.1\text{--}1\text{ }\mu\text{m}$ ) in a liquid where only the Brownian motions suspend the particles. A gel is a state where both liquid and solid are dispersed in each other, which presents a solid network containing liquid components. The sol–gel coating process usually consists of 4 steps: (1) The desired colloidal particles once dispersed in a liquid to form a sol, (2) The deposition of sol solution in a liquid to form a sol, (3) The deposition of sol solution produces the coatings on the substrates by spraying, dipping or spinning, (4) The particles in sol are polymerized through the removal of the stabilizing components and produce a gel in a state of a continuous network, (4) The final heat treatments pyrolyze the remaining organic or inorganic components and form an amorphous or crystalline coating. There are two distinct reactions in the sol–gel process: hydrolysis of the alcohol groups and condensation of the resulting hydroxyl groups. As an example, we can refer to the research done by Mohammadi et al. on a 1D coordination polymer of  $[\text{Tl}(2,4,6\text{-tcp})]_n$  (**1**). First, the precursor **1** (2 mmol) was dissolved in  $\text{H}_2\text{O}$  (30 mL) as solvent. Afterwards, PVA (1 g) was added to the solution and the solution was stirred and heated to become homogeneous (sol). Finally the sol was converted to a viscose gel. The obtained gel was calcined in a furnace by heating at  $400\text{ }^\circ\text{C}$  and  $\text{Tl}_2\text{O}_3$  nanostructure resulted. The resulting  $\text{Tl}_2\text{O}_3$  prepared by the sol–gel method in PVA has a microrods nanostructure mixed morphology (Fig. 11).



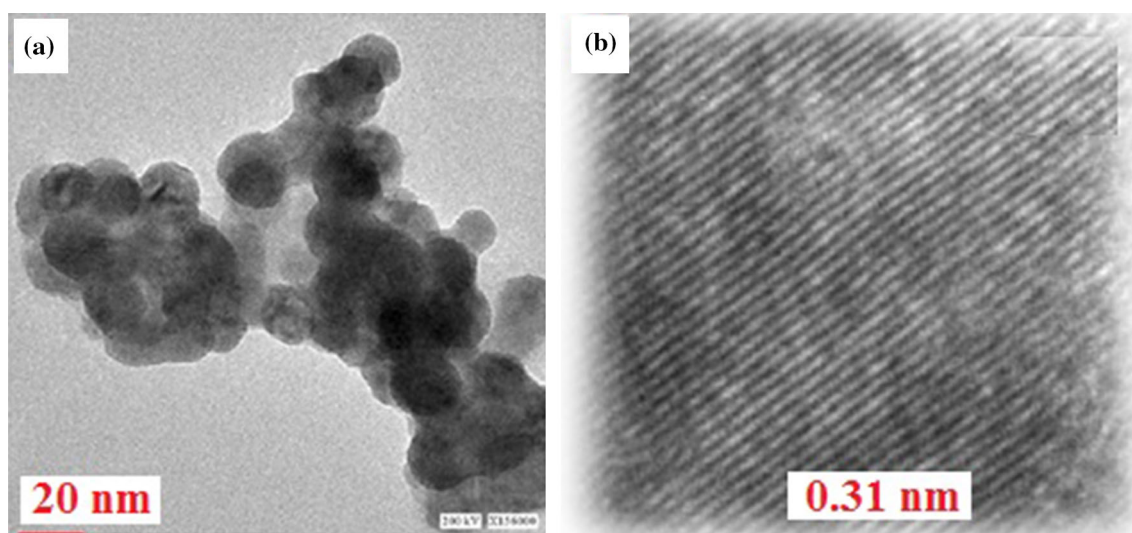


**Fig. 10** HRTEM images of **a** as-synthesized  $Tl_2O_3$  nanoparticles with a magnification of 156 000 and **b** lattice image of an individual spherical  $Tl_2O_3$  nanoparticle with a magnification of 520 000 in which

the lattice planes (222) are clearly resolved. Reproduced with permission of Royal Society of Chemistry

## 2.6 Using Potassium Superoxide

Recently, T. E. Sutto was reported a novel one-step synthesis of thallium(III) oxide nanoparticles using potassium superoxide [62]. It was demonstrated that the reaction of  $KO_2$  with different salt solutions produces grams of stable, near unit-cell sized nanoparticles [26]. In this procedure, room temperature, solution synthesis of thallium(III) oxide nanoparticles is reported with a size of about 10 nm.

## 3 Conclusions

In summary we tries to give an overview of all synthetic procedures which were reported up to now for preparation of bulk and nanostructures of thallium(III) oxide. These

methods include electrochemical methods (include electrochemical deposition and photoelectrochemical deposition), thermal method, CVD, microwave irradiation, sol-gel method and one recently chemical route using potassium superoxide. The reported electrochemical deposition process results in formation of bulk thallium(III) oxide, but by photoelectrochemical deposition process, we can prepare a thin film of thallium(III) oxide which has nanostructural surface. Thermal methods are simple and effective techniques which include thermal decomposition and calcination of various precursors. The initial precursors in thermal methods may be thallium(I) salts (e.g.  $TlBr$  or  $TlNO_3$ ) or thallium(I) supramolecular polymers. By thermal methods, we can obtain thallium(III) oxide nanoparticles, nanorods or a bulk  $Tl_2O_3$  with nanostructural surface. From different thallium(I) supramolecular polymers, different morphology of thallium(III) oxide nanostructures can be prepared. This point shows the influence of crystal packing of supramolecular polymers upon morphology and size of nano materials produced from their calcination. It seems that with increasing thermolysis or calcination temperature of thallium(I) supramolecular polymers, small nanostructures were grown and finally thallium(III) oxide nanorods were formed. In addition, thermolysis or calcination of supramolecular polymers with chloro substituted organic ligand, results in formation of thallium(I) chloride nanostructures. CVD and microwave irradiation are two other methods for synthesise of bulk and nanostructures of thallium(III) oxide, respectively. Microwave heating provides an effective and rapid method for the synthesis of nanocrystalline thallium(III) oxide powders because of its homogeneous and fast-

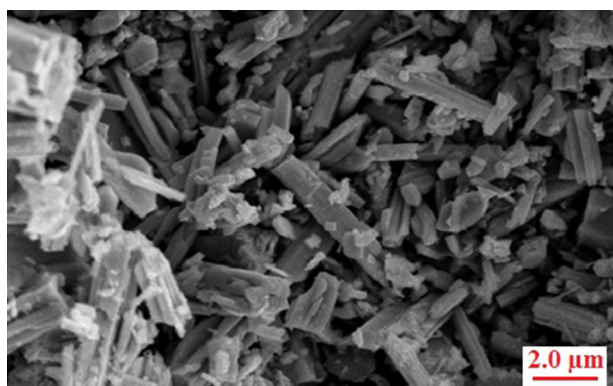


**Fig. 11** SEM micrograph of  $Tl_2O_3$  microstructure produced by sol-gel thermal decomposition of compound  $[Tl(2,4,6-tcp)]_n$  (**1**) in PVA. Reproduced with permission of John Wiley & Sons

heating characteristics. It seems that, sol–gel method is not an appropriate procedure for preparation of thallium(III) oxide nanostructures. On the other hand, a novel one-step, room temperature, solution synthesis of thallium(III) oxide nanoparticles with a size of about 10 nm is reported by using potassium superoxide.

**Acknowledgments** The authors would like to acknowledge the financial support of University of Tehran for this research under grant number 01/1/389845.

## References

- P. Pyykko, Chem. Rev. **97**, 597 (1997)
- H.M. Alvarez, P.A. Gillespie, C.D. Gause, A.L. Rheingold, J.A. Golen, D. Rabinovich, Polyhedron **23**, 617 (2004)
- C. Janiak, Coord. Chem. Rev. **163**, 107 (1997)
- C. Janiak, Main Group Met. Chem. **21**, 33 (1998)
- C. Janiak, J. Prakt. Chem. **340**, 181 (1998)
- K. Akhbari, A. Morsali, J. Mol. Struct. **878**, 65 (2008)
- D.M. Lyons, M.A. Morris, Cryst. Growth Des. **2**, 427 (2002)
- B. Notash, N. Safari, H.R. Khavasi, V. Amani, A. Abedi, J. Organomet. Chem. **693**, 3553 (2008)
- K. Akhbari, A. Morsali, Coord. Chem. Rev. **254**, 1977 (2010)
- M.S.Y. Parast, A. Morsali, Z. Anorg. Allg. Chem. **638**, 451 (2012)
- A. Morsali, M.Y. Masoumi, Coord. Chem. Rev. **253**, 1882 (2009)
- M. Mohammadi, A. Morsali, Z. Anorg. Allg. Chem. **637**, 2312 (2011)
- K. Akhbari, K. Alizadeh, A. Morsali, M. Zeller, Inorg. Chim. Acta **362**, 2589 (2009)
- M. Mohammadi, K. Akhbari, Y. Hanifehpour, A. Morsali, S.W. Joo, G. Bruno, H.A. Rudbari, J. Organomet. Chem. **733**, 15 (2013)
- S. Hunig, H. Meixner, T. Metzenthin, U. Langohr, J.U. Schutz, H.C. Wolf, E. Tillmanns, Adv. Mater. **2**, 361 (1990)
- G.S. Sivagurunathan, K. Ramalingam, C. Rizzoli, Polyhedron **65**, 316 (2013)
- H. Sabrowsky, Z. Anorg. Allg. Chem. **381**, 266 (1977)
- R. Marchand, M. Tournoux, C.R. Hebd, Seances Acad. Sci. Ser. C **277**, 863 (1973)
- P. Papamantellos, Z. Kristallogr. **126**, 143 (1968)
- G.A. Tsirlina, O.A. Petrii, J. Electroanal. Chem. **401**, 33 (1996)
- R.J. Phillips, M.J. Shane, J.A. Switzer, J. Mater. Res. **4**, 923 (1989)
- K. Wade, A. Banister, in *Comprehensive Inorganic Chemistry*, ed. by J.C. Bailar (Pergamon Press, Oxford, 1973)
- D. Cubicciotti, F.J. Kenesha, J. Phys. Chem. **71**, 808 (1967)
- A.D. Berry, R.T. Holm, R.L. Mowery, N.H. Turner, M. Fatemi, Chem. Mater. **3**, 72 (1991)
- M.S. Yazdan Parast, A. Morsali, P. Ebrahimpour, Dalton Trans. **41**, 5848 (2012)
- M. Schlesinger, Electroless and electrodeposition of silver, in *Modern Electroplating*, 5th edn., ed. by M. Schlesinger, M. Paunovic (Wiley, New York, 2010), p. 131
- W. Szczepaniak, (2005) Wydawnictwo naukowe PWN W-wa (Metody instrumentalne w analizie chemicznej)
- U. Kumar, Electrochemical methods in nanomaterials preparation, in *Sur Recent Trend in Electrochemical Science and Technology*, ed. by U. Kumar (Wiley, New York, 2012), p. 261
- K. Hnidaa, J. Mechb, G.D. Sulka, Appl. Surf. Sci. **287**, 252 (2013)
- J.F. Liu, S.X. Wang, K.Z. Yang, Thin Solid Films **298**, 156 (1997)
- R.N. Bidattacharya, P. Pramanik, Bull. Mater. Sci. **2**, 287 (1980)
- Powder diffraction file JCPDS International Centre for Diffraction Data Swarthmore PA Pattern No. 33-1404
- A.J. Bard, Lr Faulkner, Photoelectrochemistry and Electrogenerated Chemiluminescence, in *Electrochemical methods Fundamentals and Applications*, 2nd edn., ed. by A.J. Bard, M. Stratmann (Wiley, New York, 2001), p. 745
- J.A. Switzer, J. Electrochem. Soc. **136**, 1009 (1989)
- A.J. Bard, Science **207**, 139 (1980)
- A. Heller, Ace. Chem. Res. **14**, 154 (1981)
- M.Y. Masoomi, A. Morsali, Coord. Chem. Rev. **256**, 2921 (2012)
- M.Y. Masoomi, A. Morsali, RSC Adv. **3**, 19191 (2013)
- M.Y. Masoomi, A. Morsali, P.C. Junk, RSC Adv. **4**, 47894 (2014)
- M.Y. Masoomi, A. Morsali, P.C. Junk, CrystEngComm **17**, 686 (2015)
- E. Tahmasebi, M.Y. Masoomi, Y. Yamini, A. Morsali, Inorg. Chem. **54**, 425 (2015)
- M.Y. Masoomi, S. Beheshti, A. Morsali, Cryst. Growth Des. **15**, 2533 (2015)
- M.Y. Masoomi, A. Morsali, Ultrason. Sonochem. **28**, 240 (2016)
- F. Shahangi Shirazi, K. Akhbari, Inorg. Chem. Acta. **436**, 1 (2015)
- F. Shahangi Shirazi, K. Akhbari, RSC Adv. **5**, 50778 (2015)
- M. Moeinian, K. Akhbari, J. Solid State Chem. **225**, 459 (2015)
- K. Akhbari, A. Morsali, Dalton Trans. **42**, 4786 (2013)
- K. Akhbari, M. Hemmati, A. Morsali, J. Inorg. Organomet. Polym. **21**, 352 (2011)
- K. Akhbari, A. Morsali, P. Retailleau, Polyhedron **29**, 3304 (2010)
- K. Akhbari, A. Morsali, Inorg. Chem. Acta. **363**, 1435 (2010)
- R. Bashiri, K. Akhbari, A. Morsali, Inorg. Chem. Acta. **362**, 1035 (2009)
- M. Mohammad, A. Morsali, Mater. Lett. **63**, 2349 (2009)
- M.J. Soltanian Fard, S. Tabaroki, Mater. Sci-Pol **32**, 23 (2014)
- K. Akhbari, A. Morsali, Polyhedron **30**, 1456 (2011)
- K. Akhbari, A. Morsali, Polyhedron **30**, 2459 (2011)
- K. Akhbari, A. Morsali, J. Organomet. Chem. **700**, 125 (2012)
- K. Akhbari, A. Morsali, CrystEngComm **14**, 1618 (2012)
- M. Mohammadi, K. Akhbari, A. Mazloomifar, A. Ramazani, A. Morsali, G. Bruno, H.A. Rudbari, J. Inorg. Organomet. Polym. **22**, 288 (2012)
- J.R. Creighton, P. Ho, Introduction to Chemical Vapor Deposition (CVD), in *ASM International*, ed. by J.H. Park (ASM International, Materials Park, 2001), p. 1
- R. Sanghi, Resonance. **77** (2000)
- C.R. Patra, A. Gedanken, New J. Chem. **28**, 1060 (2004)
- T.E. Sutto, Inorg. Chem. **53**, 4570 (2014)